

Relativistic N - N one-boson-exchange potentials with asymptotic power-law energy dependence

T. Ueda* and A. E. S. Green

University of Florida, Gainesville, Florida 32611

(Received 7 October 1977; revised manuscript received 6 March 1978)

We update the relativistic version of the generalized one-boson-exchange potentials on the basis of the recent accumulation of experimental data. We introduce into the vector-meson potentials a damping factor decreasing with energy as well as an enhancing factor in the scalar-meson potential increasing with energy in accord with the asymptotic power-law energy dependence of the potentials required in high-energy physics. With these factors we obtain a markedly improved fit to all phase parameters. Thus, with 11 adjusted parameters we obtain a satisfactory description of the N - N interaction for the 0–515 MeV energy range.

NUCLEAR STRUCTURE Relativistic one-boson-exchange potentials with asymptotic power-law energy dependence. Theoretical fits to phase shifts and observables.

I. INTRODUCTION

Recently considerable progress has been made in experimental measurements of the nucleon-nucleon system in the 0–50 MeV region as well as in the 200–500 MeV region.¹⁻³ These data have reduced the error bars of the phase parameters⁴⁻⁶ to approximately one-half of those obtained 10 years ago.^{7,8}

Using this new experimental information, this paper presents an updated version of our relativistic generalized one-boson-exchange potential (OBEP) for the energy range of 0–515 MeV. The generalized meson field theory work^{9,10} by one of us (A.G.) embodying what has subsequently been referred to as “regularization” and containing a combination of vector, scalar, and pseudoscalar meson fields is one basis of our approach. The approximate cancellation of the large static interactions generated by vector- and scalar-meson fields gives major importance to the residual relativistic terms which are tractable with regularization. These physical features are maintained in current models.

The early one-boson-exchange model studies¹¹⁻¹³ for the intermediate and outer region of the force range by one of us (T.U.) and others is the other initial basis of our OBEP approach. Subsequent developments of the OBEP with regularization or the use of meson form factors have led to realistic nonrelativistic¹⁴⁻¹⁶ and relativistic models^{17,18} including one by Ueda, Nack, and Green (UNG)¹⁸ which covers the energy region of 0–1000 MeV using a complex potential. These together with the dispersion theoretical¹⁹ and the K -matrix approach²⁰ for the 0–3 GeV energy range by one of us (T.U.) are our basis for the inelastic region. In ad-

dition to the work at Florida and Osaka, groups at Texas A & M, M.I.T., Nijmegen, Beer-sheva, Bonn, Paris, and Stony Brook have also pursued similar boson exchange models. For reviews of these works we refer the reader to the Proceedings of the First and Second International Conferences on the Nucleon-Nucleon Interaction^{21,22} as well as Refs. 12 and 13.

In addition to updating earlier models in UNG,¹⁸ we here introduce (i) a damping factor decreasing with energy which multiplies the vector-meson-exchange potentials and (ii) an enhancement factor increasing with energy which multiplies the scalar-meson-exchange potentials. The first modification is based on our view that the vector-meson-exchange amplitude should tend to the Reggeized vector-meson-exchange amplitude at very high energies. Actually one of us (T.U.) showed already that the one-boson-exchange amplitude with a similar modification works well at very high energies²³ and interpreted this modification in terms of the bilocal-field exchange²⁴ or equivalently the exchange of an infinite series of mesons between the two nucleons. The second modification is based on the following view and is intended to improve fits of the model to data. The $I=0$ scalar-meson exchange can be interpreted as the $I=J=0$ part of the two-pion exchange with a nucleon and a Δ in the intermediate states.²⁵ Therefore, there is a possibility that at energies beyond the one pion production threshold, the Δ production increasing with energy produces some enhanced correction in the scalar-meson-exchange amplitude. Secondly, we have a possibility that tensor-meson-exchange contributions, which are in part similar to the scalar-meson contribution,¹⁹ may be incorporated by this enhancement factor, because the tensor-meson-

exchange amplitude increases with energy with a factor proportional to the square of the laboratory energy relative to the scalar-meson-exchange amplitude.

These two modifications produce remarkable improvements in fits of our model to the data. With the introduction of only one additional parameter to describe these factors, we reduce the χ^2 value to $\frac{2}{3}$ of that of the unmodified model.

Perhaps it should also be mentioned at the onset that recent data have exposed some defects of the old phase parameters. For example, the D_i parameter from np scattering data at 325 MeV, provided by recent measurements at TRIUMPH,¹ deviate considerably from the predictions of the Livermore X solution.⁷ In addition, a new measurement of the A_{yy} parameter from np scattering data at 50 MeV has led to the conclusion that the ϵ_1 parameter given in the Livermore analyses has been persistently too negative. Since most potentials, either theoretical or phenomenological, have been constructed referring to the old phase parameters, especially the Livermore X solution, we believe that it is worthwhile to present new potentials based on the new data. The new potentials have manifest improvements over the last relativistic potentials having χ^2 values of $\frac{1}{3}$ – $\frac{1}{4}$ of the old ones.¹⁸

In Sec. II we describe definitions and basic equations. In Sec. III our models are explained. In Sec. IV the data for the χ^2 test are given. Numerical results are given in Sec. V. We give also some variations of our models in Sec. VI and results on observables in Sec. VII. In Sec. VIII we compare our work with other recent potentials, discuss related problems, and present our conclusions.

II. FORMALISM

The basic equations used in this paper are described in our previous papers.^{17,18} For definiteness for the spin singlet case the basic equation is

$$K(\vec{p}, \vec{k}) = V(\vec{p}, \vec{k}) + \int_0^\infty q^2 d\vec{q} V(\vec{p}, \vec{q}) G(\vec{q}, \vec{k}) K(\vec{q}, \vec{k}), \quad (1)$$

where \vec{p} and \vec{k} are the final and initial c.m. momentum of the scattered nucleon, respectively, $V(\vec{p}, \vec{q})$ is the OBEP in the momentum space, and $G(\vec{q}, \vec{k})$ is a two-nucleon propagator given by

$$G(\vec{q}, \vec{k}) = P \{ 4\pi^3 m^2 / E^2(\vec{q}) [E(\vec{q}) - E(\vec{k})] \}, \quad (2)$$

where $E(\vec{k}) = (\vec{k}^2 + m^2)^{1/2}$, m is the nucleon mass, and P denotes the principal value. $K(\vec{p}, \vec{k})$ which is determined by Eq. (1) is related to the S matrix by means of

$$S = (1 + iK/\pi\rho) / (1 - iK/\pi\rho), \quad (3)$$

where $\rho = E(\vec{k})/k$. The partial wave projection of Eq. (1) gives

$$K_l(p, k) = V_l(p, k) + \int_0^\infty q^2 dq V_l(p, q) G(q, k) K_l(q, k), \quad (4)$$

where l denotes the orbital angular momentum and p , k , and q represent the magnitudes of \vec{p} , \vec{k} , and \vec{q} , respectively. K_l is now related to the phase shift δ as follows:

$$K_l(p, p) = \tan \delta_l(p) / \pi \rho(p). \quad (5)$$

The OBEP $V_l(p, q)$ have been derived in Refs. 11 and 12 on the nucleon mass shell and are represented for the scalar and pseudoscalar potentials, respectively, as follows:

$$V_l^{(S)}(p, k) = q_s^2 C(\beta_- - Z) Q_l(Z), \quad (6.1)$$

$$V_l^{(P)}(p, k) = g_p^2 C(Z - \beta_+) Q_l(Z). \quad (6.2)$$

In Eqs. (6.1) and (6.2) Q_l is the second kind of Legendre function and C , β_\pm , and Z are defined by

$$C = 1 / [2(2\pi)^5 m^2],$$

$$\beta_\pm = \frac{E(p) + m}{E(k) \pm m} \frac{k}{2p} + \frac{E(k) \pm m}{E(p) + m} \frac{p}{2k},$$

$$Z = (k^2 + p^2 + \mu^2) / (2kp),$$

where μ is the meson mass. The vector-meson-exchange potential is complicated and only the expression on the nucleon mass shell ($p = k$) is shown as follows:

$$\begin{aligned} V_l^{(V)}(p, p) &= (g_v + 2f_v)^2 \frac{C}{2\epsilon} (1 + 6\epsilon + \epsilon^2) Q_l(Z) - 2(g_v + 2f_v) \\ &\quad \times f_v \frac{C}{\epsilon} [2E - m + 2\epsilon Z - (2E + m)\epsilon^2] Q_l \\ &\quad + f_v^2 \frac{C}{m^2 \epsilon} (3p^2 + 2m^2 Z)(1 + \epsilon^2 - 2\epsilon Z) Q_l, \end{aligned} \quad (6.3)$$

where $\epsilon = p^2 / (E + m)^2$. In Eqs. (6.1), (6.2), and (6.3) we ignored the terms with δ_{l0} which disappear after the regularization described later.

The interaction Hamiltonian densities leading to these potentials are as follows:

$$H_P = g_P \bar{\psi}(p) i\gamma_5(\vec{q}) \phi^P(k),$$

$$H_S = g_S \bar{\psi}(\vec{p}) \psi(\vec{q}) \phi^S(\vec{k}),$$

$$H_V = g_V \bar{\psi}(\vec{p}) i\gamma_\mu \psi(\vec{q}) \phi_\mu^V(\vec{k})$$

$$+ i \frac{f_V}{2m} \bar{\psi}(\vec{p}) \sigma_{\mu\nu} \psi(\vec{q}) [k_\mu \phi_\nu^V(\vec{k}) - k_\nu \phi_\mu^V(\vec{k})],$$

where $\vec{k} = \vec{p} - \vec{q}$, $\sigma_{\mu\nu} = (\gamma_\mu \gamma_\nu - \gamma_\nu \gamma_\mu) / 2i$.

The potentials of Eqs. (6.1), (6.2), and (6.3) are for the case without form factors at the meson-nucleon vertices. In this paper we assume the following form factor:

$$F(k^2) = \left(\frac{\Lambda^2}{k^2 + \Lambda^2} \right)^2, \quad (7)$$

which gives in turn the quadrupole regularization of the potentials. This procedure of the regularization is described in one of our previous papers.¹⁶ For numerical calculations we use the regularized potential represented by the sum of the expressions of Eqs. (6.1) to (6.2) as follows:

$$V_i = \frac{1}{\Lambda_0^2} \sum_{j=0}^4 \left(\prod_{i=0}^4 \frac{\Lambda_i^2}{-\Lambda_j^2 + \Lambda_i^2} \right) V_i(\Lambda_j), \quad (8)$$

where π' denotes the product except $i=j$, $\Lambda_0 = \mu$, $\Lambda_j = [1 + (j-1)/100] \Lambda$ with $j=1, \dots, 4$, $V_i(\Lambda_j)$ is represented by Eqs. (6.1) to (6.3) with μ replaced by Λ_j .

We note here for later use the high-energy behavior of the potentials in Eq. (1). The scalar potential behaves with a fixed t and s approaching infinity as

$$V^{(S)}(s, t) \rightarrow \text{constant}, \quad (9.1)$$

where $s = (2E)^2$ and $t = 2p^2(1 - \cos\theta)$; θ is the c.m. scattering angle, while the vector potential behaves as

$$V^{(V)}(s, t) \rightarrow s. \quad (9.2)$$

On the other hand, the Reggeized vector and the Reggeized tensor potentials behave with $t=0$ as

$$\tilde{V}^{(V)}(s, t) \rightarrow s^{\alpha_V(t)} \simeq \sqrt{s}, \quad (9.3)$$

$$\tilde{V}^{(t)}(s, t) \rightarrow s^{\alpha_t(t)} \simeq \sqrt{s}. \quad (9.4)$$

These features, i.e., the power-law behavior, are taken into account in the next section.

III. MODELS

The mesons used in this paper are the same as those of UNG,¹⁸ i.e., the π , ρ , ω , δ , S^* , σ , and η . The observed mass values are used for these mesons except the σ . The mass of σ is assumed to be 352 MeV, the same value as that of UNG.

Model I. This model is an updated version of that of UNG which is made by fitting the new data described in Sec. IV. Ten parameters are used: the seven coupling constants of the mesons, the tensor to vector coupling constant ratio for ρ , the π regulator Λ_π , and the regulator Λ common to the residual mesons. In Sec. VI two variations of this model are discussed.

Model II. In this model we introduce the damping factor decreasing with energy by which the ω and ρ exchange potentials $V_i^{(V)}(p, q)$ are multiplied. The factor is assumed to be

$$D(p, q) = 1 / [(1 + p/\Omega_V)(1 + q/\Omega_V)]^{1/2}, \quad (10)$$

with a parameter Ω_V .

As seen from the argument in Sec. II, the regularized $V_i^{(V)}(p, q)$, multiplied by this factor, satisfies the power-law behavior of the ω and ρ Regge-trajectory exchange amplitudes which are now established at high energies. This model has 11 parameters including Ω_V .

Model III. In this model we introduce the enhancement factor increasing with energy which multiplies the S^* , σ , and δ exchange potentials $V_i^{(S)}(p, q)$,

$$E(p, q) = [(1 + p/\Omega_S)(1 + q/\Omega_S)]^{1/2} \quad (11)$$

with a parameter Ω_S . This factor may be interpreted as a correction from the tensor-meson-exchange contribution as stated in Sec. I; or the $V_i^{(S)}(p, p)$ multiplied by this factor corresponds correctly to the power-law behavior of the f_0 and A_2 Regge-trajectory exchange amplitudes which are well established at high energies. This model also has 11 parameters including Ω_S .

Model IV. This model is a combination of model II with model III. $D(p, q)$ and $E(p, q)$ simultaneously multiply the vector-meson and the scalar-meson exchange potentials, respectively, with $\Omega_V = \Omega_S$. This model again has 11 parameters. A variation of this model is discussed in Sec. VI.

IV. PHASE PARAMETERS FOR COMPARISON

Fits of our models to data are judged on the three points: the low energy parameters, the χ^2 test described below for the 25–35 MeV energy range and the comparisons in phase parameters and some observables at 425 and 515 MeV.

The χ^2 of the models are determined using 72 phase parameters with $J=0, 1$, and 2 at 25, 50, 100, 150, 200, and 325 MeV. The χ^2 value is defined by

$$\chi^2 = \sum_{i=1}^{72} \left(\frac{\delta_t^i - \delta_e^i}{\Delta_e^i} \right)^2, \quad (12)$$

where δ_t^i , δ_e^i , and Δ_e^i are the theoretical and experimental phase parameters and the experimental error bar, respectively. We use the most recent available results of phase shift analyses for the χ^2 test. At 50 MeV, we use the phase parameters by Arndt except ϵ_1 and $\delta(^1P_1)$. For these two we combine Arndt's phase parameters⁵ with Singnell's,⁶ both involving the recent experimental results on A_{yy} by the Davis group.³ The combination procedure is as follows. Suppose two phase parameters are $X_1 \pm \Delta_1$ and $X_2 \pm \Delta_2$, then the combined X and Δ are defined by

$$X = \frac{1}{2} (\text{Max}\{X_1 + \Delta_1, X_2 + \Delta_2\} + \text{Min}\{X_1 - \Delta_1, X_2 - \Delta_2\}), \quad (13)$$

$$\Delta = \frac{1}{2} (\text{Max}\{X_1 + \Delta_1, X_2 + \Delta_2\} - \text{Min}\{X_1 - \Delta_1, X_2 - \Delta_2\}).$$

At 325 MeV we combine Arndt's phase parameters⁵ with Edgington's,¹ both involving recent experimental results on the triple scattering parameters in TRIUMPH.¹ For Edgington's $I=0$ phase parameters we use the number 1 solution as this set is in better accord with OBEP predictions for 3G waves. For these high partial waves OBEP predictions should be reliable. At other energies we use the energy-independent solution of the phase parameters by Arndt, Hackman, and Roper (AHR).⁴ The phase parameters for the χ^2 test are given in an appendix.

We use combinations of phase parameters by the different authors for the following reasons. The two sets of phase parameters are only a little different from each other. Thus their error bars overlap except for $\delta({}^1P_1)$ at 325 MeV. Both sets involve the recent experimental results and equally well reproduce all available data. At present it is difficult to decide which is more likely to be correct.

At 425 and 515 MeV we use Edgington's⁷ result for the $I=1$ phase parameters and the energy-dependent solution of AHR⁴ for the $I=0$ phase parameters.

In the present calculation we ignore all the electromagnetic corrections. Since the $I=1$ phase parameters described above are obtained for proton-proton scattering, we subtract the electromagnetic contributions from the $I=1$ phase parameters for comparison with our calculation. These contributions are assumed to be the difference between the proton-proton and neutron-proton phase parameters given by the energy-dependent solution in AHR.⁴

The models in this paper are intended to fit data over the entire energy region from 0 to 515 MeV, including the deuteron binding energy. In view of the great importance of the three phase parameters, $\delta({}^1S_0)$, $\delta({}^3S_1)$, and ϵ_1 for problems of nuclear

binding, we emphasize the fits of these parameters with a technique described in an appendix. We make no explicit calculation of the deuteron quadrupole moment in this paper; however, we implicitly have a fit to the quadrupole moment by fitting ϵ_1 and $\delta({}^3S_1)$ parameters at very low energies. The searches on the model parameters were first made at energies of 1, 25, 150, and 325 MeV. However, to obtain good fits over the entire energy range, we use a technique described in the appendix.

V. NUMERICAL RESULTS

The model parameters are shown in Table I. The χ^2 test results, the low energy parameters, and the deuteron binding energy are given in Table II. The deuteron binding energy is estimated from the values of the scattering length and the effective range in the 3S_1 state. Fits in models II, III, and IV are quite similar in all respects. Thus we chose model IV as the representative of the three models, since model IV has features averaged over models II and III. We compare our results for models IV and I with the phase shift analysis results at 0–515 MeV for Fig. 1, and show numerical values of the phase parameters in models IV up to 970 MeV in Table III. In the inelastic energy region we ignored the imaginary component of the potentials. In UNG¹⁸ we calculated the effect of the imaginary component on the phase parameters at 660 and 970 MeV and the effects are found to be rather small in states where no inelastic resonance exists. Thus the present theoretical predictions for the inelastic energy region are expected to serve as a good approximation except for the 1D_2 and 3F_3 states where resonances may exist.²⁶⁻²⁸

In UNG the χ^2 values for solutions 1 and 2 are 1434 and 1101, respectively. Therefore model I with $\chi^2=530$ is a considerable improvement over the UNG models. Furthermore, as seen in Fig. 1,

TABLE I. Model parameters.

Meson	Mass (MeV)	I g^2	II g^2	III g^2	IV g^2
π	138.7	14.17	14.83	14.85	14.86
ρ	759.1	0.4555	0.2611	0.2672	0.2425
$(f/g)_\rho$		6.104	8.978	8.592	9.155
ω	782.8	9.342	11.92	12.15	12.05
δ	970.0	1.466	1.037	1.276	1.075
S^*	993.0	14.67	15.87	15.28	15.60
σ	352.0	0.8566	1.097	1.111	1.109
η	548.8	4.512	4.389	4.618	4.452
Λ_π (MeV)		3601.9	4075.9	8185.6	4874.8
Λ (MeV)		1698.4	1834.8	1847.5	1861.7
Ω (MeV)			3279.7	3207.0	6567.3

TABLE II. The test of models. The scattering length a and the effective range r are given in units of fm for the cases of the spin singlet s and the spin triplet t . E_d is the deuteron binding energy in units of MeV.

Model	χ^2	$(\chi^2/\text{data})^{1/2}$	a_s	r_s	a_t	r_t	E_d
I	530	2.7	-23.6	2.68	5.47	1.80	2.2
II	327	2.1	-24.3	2.57	5.47	1.79	2.2
III	359	2.2	-23.7	2.44	5.45	1.79	2.2
IV	328	2.1	-23.9	2.51	5.48	1.79	2.2
Experiment			-23.7	2.73	5.41	1.71	2.22

the fits of model IV are quite satisfactory up to 325 MeV with $\chi^2=328$ and the improvements of the fits in model IV, compared with those in model I, are apparent. The deviations in model I in the 1D_2 and 3D_2 states at 325 MeV are greatly reduced in model IV.

At 515 MeV we recognize considerable discrepancies between our prediction in model IV and the data for the 1D_2 , 1F_3 , ϵ_1 , and 3F_3 phase parameters. The discrepancies in the 1D_2 and 3F_3 phase parameters may be connected with a possible quasibound state in the 1D_2 state²⁶ at about 600 MeV and an inelastic resonance in the 3F_3 state at about 800 MeV.²⁷ Recently one of us (T.U.) has explained

the existence of the quasibound state and the resonance in terms of πNN dynamics.²⁶ As for the discrepancies in the 1F_3 and ϵ_1 parameters, it is not clear whether this really implies something beyond the OBEP model or uncertainties inherent in the phase shift analyses, because the experimental information is insufficient.

At 325 MeV model IV gives quite satisfactory fits to the newest phase shift parameters of Arndt.⁵ The parameters use inputs from the most recent experimental data from meson factories.^{1,2} The 3P_2 phase parameter in model IV at 325 MeV is a little larger than those of Arndt's and Edgington's data; however, we have a good fit to the data at

TABLE III. The phase parameters of model IV.

Energy	1.00	5.00	10.00	25.00	50.00	100.00	150.00	200.00	325.00	425.00	515.00	660.00	970.00
1S_0	62.55	64.26	60.58	51.58	41.11	26.95	16.67	8.35	-7.85	-18.08	-26.00	-37.01	-55.87
3P_0	0.23	2.05	4.61	10.24	13.36	10.73	5.40	-0.09	-12.15	-19.91	-25.70	-33.12	-42.79
1P_1	-0.20	-1.59	-3.24	-6.72	-10.31	-15.53	-20.11	-24.32	-33.10	-38.84	-43.05	-48.33	-55.81
3S_1	147.42	117.53	101.72	79.45	61.08	40.93	28.06	18.50	0.67	-9.96	-18.04	-29.19	-48.29
3P_1	-0.12	-1.05	-2.26	-5.23	-8.78	-14.11	-18.53	-22.43	-30.59	-35.93	-40.10	-45.86	-55.72
3D_1	-0.01	-0.20	-0.74	-3.01	-6.81	-12.67	-16.69	-19.37	-23.32	-24.50	-24.95	-25.31	-27.03
E_1	0.12	0.74	1.28	1.98	2.40	2.96	3.61	4.52	6.45	8.07	9.32	10.86	12.47
1D_2	0.00	0.05	0.19	0.80	1.95	4.15	5.97	7.34	8.92	8.75	7.87	5.56	-1.14
3P_2	0.03	0.31	0.86	2.96	6.46	11.70	15.16	17.63	21.33	22.51	22.60	21.42	16.10
3D_2	0.01	0.24	0.94	4.20	10.34	19.97	25.26	27.50	26.67	23.35	19.71	13.48	0.64
3F_2	0.00	0.00	0.01	0.12	0.40	0.99	1.39	1.53	0.66	-1.05	-3.09	-6.98	-16.16
E_2	-0.00	-0.06	-0.22	-0.89	-1.89	-3.01	-3.30	-3.14	-1.98	-0.98	-0.24	0.61	1.45
1F_3				-0.44	-1.18	-2.23	-2.89	-3.43	-4.96	-6.55	-8.24	-11.26	-18.14
3D_3				0.13	0.58	2.06	3.62	4.89	6.52	6.56	5.97	4.26	-0.76
3F_3				-0.24	-0.70	-1.51	-2.14	-2.68	-4.01	-5.19	-6.34	-8.31	-12.71
3G_3				-0.06	-0.27	-0.98	-1.81	-2.64	-4.29	-5.07	-5.39	-5.25	-3.18
E_3				0.60	1.74	3.78	5.22	6.17	7.30	7.53	7.49	7.18	5.95
1G_4				0.04	0.17	0.48	0.81	1.15	1.94	2.48	2.86	3.25	3.19
3F_4				0.03	0.16	0.64	1.25	1.86	3.07	3.68	3.98	4.11	3.40
3G_4				0.18	0.78	2.40	4.08	5.63	8.76	10.40	11.26	11.64	9.55
3H_4				0.00	0.03	0.12	0.26	0.41	0.76	0.92	0.93	0.66	-1.10
E_4				-0.05	-0.20	-0.57	-0.91	-1.20	-1.69	-1.91	-2.00	-2.00	-1.64
1H_5				-0.03	-0.17	-0.56	-0.91	-1.18	-1.60	-1.83	-2.03	-2.46	-3.97
3G_5				-0.01	-0.05	-0.13	-0.16	-0.13	0.11	0.36	0.57	0.84	1.03
3H_5				-0.02	-0.09	-0.31	-0.54	-0.75	-1.13	-1.37	-1.57	-1.91	-2.81
3I_5				-0.00	-0.02	-0.13	-0.29	-0.47	-0.95	-1.29	-1.56	-1.88	-2.06
E_5				0.04	0.22	0.77	1.36	1.90	2.98	3.61	4.03	4.50	4.88

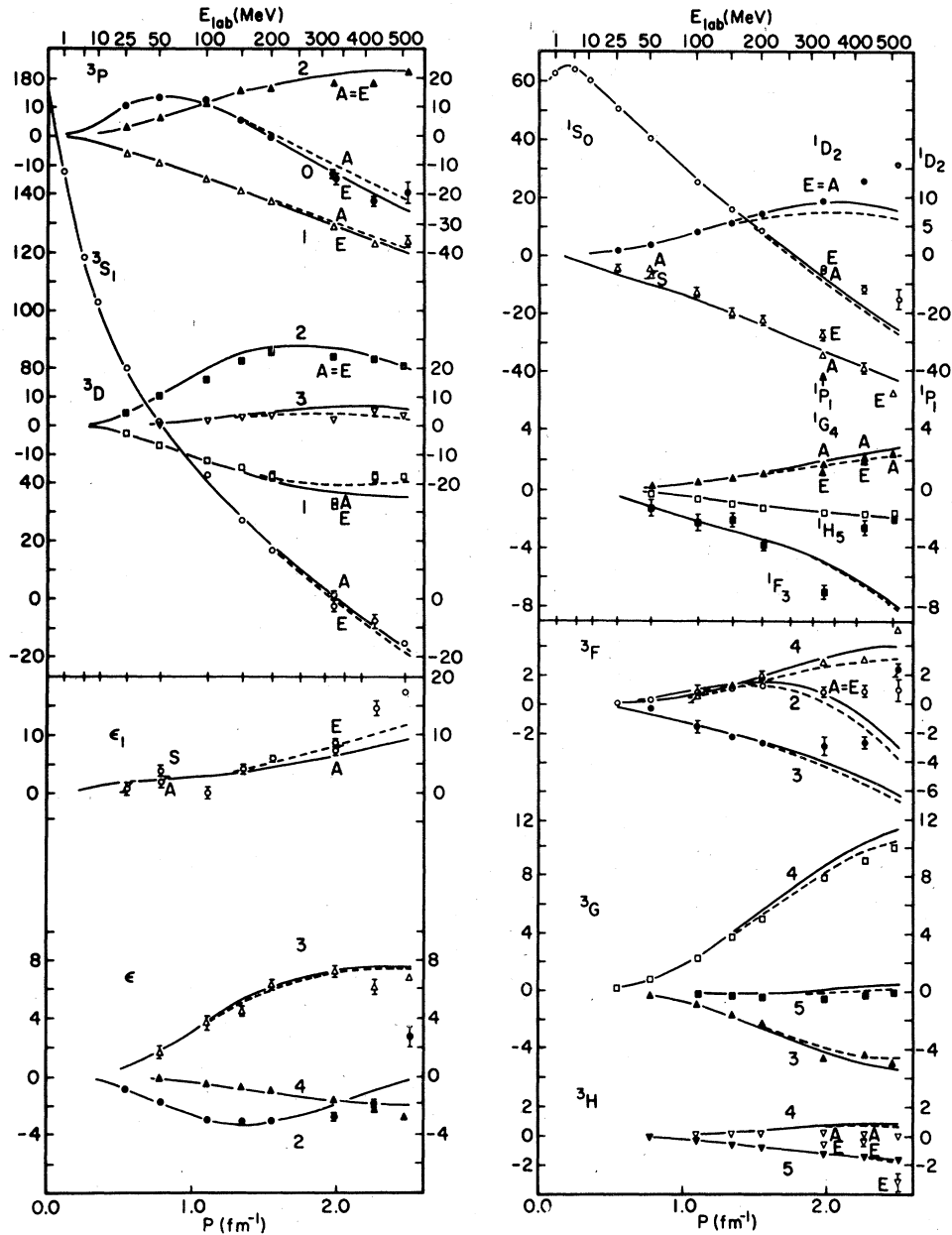


FIG. 1. Fits of models I and IV to the N - N phase parameters over $E_{\text{lab}} = 0, 515$ MeV. Model IV (I) with 11 (10) parameters corresponds to the solid (broken) curves. Only the solid curves are shown, if the broken curves are not appreciably different from the solid ones. See Sec. IV on the data from the phase shift analyses. A, E, and S denote the data from Refs. 5, 1, and 6, respectively.

515 MeV.

At 50 MeV the fits of model IV to the combined phase parameters of Arndt's⁵ and Signell's⁶ are perfect in all states except the 1P_1 state. For the 1P_1 state we predict $\delta(^1P_1) = -10.3^\circ$, compared with Arndt's $-4.81^\circ \pm 0.64^\circ$ (Ref. 5) and Signell's $-5.8^\circ \pm 1.1^\circ$.^{3,6}

The coupling constants of ρ and ω in our models are compared with the predictions from the analyses of the electromagnetic form factor²⁹

$$g_\rho^2 = 0.52_{-0.06}^{+0.07}, \quad g_\omega^2 = 4.67_{-0.81}^{+1.24}, \quad g_\phi^2 = 3.04_{-0.66}^{+1.07},$$

$$(f/g)_\rho \approx 3.6, \quad f_\omega/g_\omega \approx 0.$$

The comparison tells us that g_ω^2 in our models is considerably larger than that of the electromagnetic form factor. We interpret this as follows. Our ω represents the total effective $I=0$, $J=1$ exchange between two nucleons; that is, it corresponds to the sum of the uncorrelated 3π exchange, the uncorrelated π - ρ exchange, and other possible exchanges, all having the same quantum number as the actually observed ω meson. Apart from the correlated 3π exchange, the mass distributions of the exchanged system may be broad. However, what we use is the potential which is derived by integration over the mass variable. Therefore it can be a good mathematical approximation to replace the broad mass distributions by an appropriate sum of δ -function distributions. We use five δ functions for ω , corresponding to the ω pole and four poles for the regularization. In addition to this we note the situation that a change of the ω mass (782.8 MeV) to, for example, 700 MeV does not make an appreciable change in the resulting phase parameters, if an appropriate renormalization of the coupling constant is made.

Returning to the problem of the coupling constant difference between the electromagnetic form factor and N - N cases, we note that the values in Eq. (14) are derived with use of the photon-vector-meson coupling strengths which are evaluated from the data of leptonic decays of the actual observed vector mesons. The observed ω corresponds primarily to the correlated 3π exchange. Therefore most parts of the uncorrelated 3π and π - ρ exchanges in the N - N case do not correspond with the ingredients of the electromagnetic form factor. We think the coupling constant difference may arise for this reason.

Similarly, the fact that our $(f/g)_\rho$ is larger than those obtained from electromagnetic form factor analysis should be interpreted to mean that the uncorrelated 2π exchange with $I=J=1$ is involved in our N - N models in a different way from the case for the electromagnetic form factor. We also find that our g_η^2 of 4.5–4.6 is larger than the value $g_\eta^2 < 0.002$ (Ref. 30) obtained from other reactions. We point out the possibility that our η represents the combined effects of the observed η , the uncorrelated 3π with $I=J=0$, and the η' with mass 958 MeV.

VI. VARIATIONS OF MODEL I AND IV

Model I'. We studied the same model as model I except the mass of δ is assumed to be 560 MeV, the 4π mass. This model is interesting in that the two deviations from the data in the 1D_2 and 3D_2 phase parameters at 325 MeV may be simultaneously remedied by the isovector scalar-meson

exchange contribution with much lighter mass than the observed mass of δ . If the uncorrelated 4π exchange with the same quantum number as δ is appreciable, the effective mass of δ can be lighter than the observed δ mass, 970 MeV. Therefore, we take the lowest possible value, 560 MeV, for the effective δ mass. Model I' is found to be a considerable improvement over model I with $\chi^2=504$ and gives good fits similar to those of model I to the low energy parameters and the deuteron binding energy. Therefore, we suggest here the possibility that uncorrelated 4π exchange with $I=1$, $J=0$ may contribute considerably with lighter effective mass than the observed δ mass. The following are the parameters for model I':

$$g_\tau^2 = 14.76, \quad g_\rho^2 = 0.4853, \quad (f/g)_\rho = 6.109, \quad g_\omega^2 = 9.116, \\ g_\delta^2 = 0.5203, \quad g_{S^*}^2 = 14.75, \quad g_\sigma^2 = 0.7782, \quad g_\eta^2 = 3.006, \\ \Lambda_\tau = 3330.7 \text{ MeV}, \quad \Lambda = 1698.0 \text{ MeV}.$$

Model I''. In this model we replace the quadrupole regularization in model I by the double-dipole regularization for π , ρ , and ω , though the same quadrupole regularizations are used for the remaining mesons. The double-dipole regularizations are assumed to be

$$[F(k^2)]^2 = \left(\frac{\Lambda_1^2}{k^2 + \Lambda_1^2} \right)^2 \left(\frac{\Lambda_2^2}{k^2 + \Lambda_2^2} \right)^2, \quad (14)$$

where Λ_2 's are fixed to $4m$ and $2m$ for π and ω and ρ , respectively and Λ_1 's are searched distinctively for π , ω , and ρ . In model I'' we find $\chi^2=600$ with good fits to the low energy parameters and the deuteron binding energy. However, we do not find any advantage of model I'' over model I.

Model IV'. This model is the same as model IV except that the different functions are assumed for D and E as follows:

$$D(p, q) = \left\{ \left[1 + \left(\frac{p}{\Omega} \right)^2 \right] \left[1 + \left(\frac{q}{\Omega} \right)^2 \right] \right\}^{-1/4}, \\ E(p, q) = 1/D(p, q). \quad (15)$$

The results in this model are quite similar to those of model IV with $\chi^2=355$ and similarly good fits to the low energy parameters and the deuteron binding energy. The parameters are as follows:

$$g_\tau^2 = 14.53, \quad g_\rho^2 = 0.2201, \quad (f/g)_\rho = 9.222, \quad g_\omega^2 = 11.50 \\ g_\delta^2 = 1.039, \quad g_{S^*}^2 = 15.35, \quad g_\sigma^2 = 1.098, \quad g_\eta^2 = 4.301, \\ \Lambda_\tau = 5539.0 \text{ MeV}, \quad \Lambda = 2049.1 \text{ MeV}, \quad \Omega = 1343.0 \text{ MeV}.$$

VII. OBSERVABLES

Our theoretical results from model IV for observables are compared with data in Fig. 2. The pp data at 515 MeV and the np data at 325 MeV are

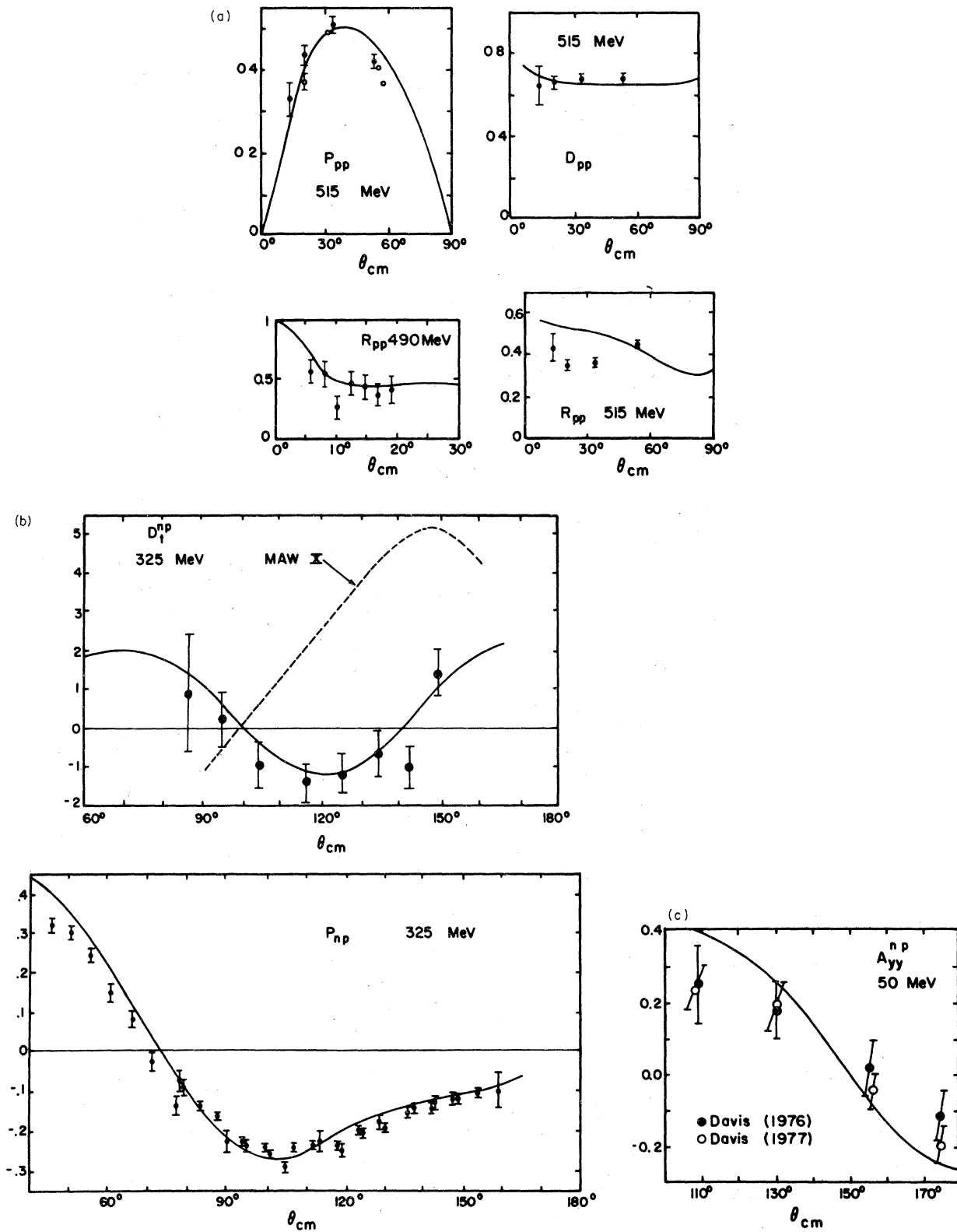


FIG. 2. Observables at 515, 490, 325, and 50 MeV as predicted by model IV. The observables illustrated at the indicated energies are polarization, P , depolarization, D_{pp} , spin rotation, R , and second spin rotation A .

provided by TRIUMPH.¹ The pp data at 490 MeV and the np data at 50 MeV are given by the Swiss Institute for Nuclear Research (SIN)² and by the Davis group,³ respectively. For calculation of the pp observables we use the inelasticities only in the 1D_2 state which are given in AHR.⁴ We find in the comparison at 515 MeV that consistency between our prediction and the data is satisfactory except for the R_{pp} parameter. However, we find in the comparison of our R_{pp} parameter with those of the SIN data at 490 MeV that our fits to the data are satisfactory.

Our fits in the P and D_t parameters for the np scattering at 325 MeV are satisfactory. In particular we have good fits to the D_t parameter, compared with those of the 1969 Livermore X phase parameters (MAWX) which were difficult to fit. This obviously suggests that theoretical models adjusted by fitting to these Livermore phase parameters would, at the very least, need some parameter readjustments.

We also compare at 50 MeV our result with the A_{yy} data given by the Davis group.³ We find that the gross features of our result are consistent with their data.

VIII. DISCUSSION

In the previous sections we have shown that model I, the updated version of the UNG model, gives $\chi^2 = 530$ [$(\chi^2/\text{data})^{1/2} = 2.7$] with 10 parameters. The introduction of the energy-damping factor and the energy-enhancement factor brings a considerable improvement to model I with $\chi^2 = 328$ [$(\chi^2/\text{data})^{1/2} = 2.1$] in model IV with 11 parameters.

This χ^2 value may be compared with that of the Paris potential³¹ which we estimate approximately to be $\chi^2 = 554$ when tested with the updated phase parameters. This potential is currently popular with its dispersion theoretical 2π exchange and its use of other established mesons. The description employs 14 parameters for the region of interparticle distance $r < 0.8-1.0$ fm as well as two coupling constants. We note that their 2π exchange calculation leads to considerable uncertainty, depending on the choice of the πN scattering data, especially in the 3P_2 state. Furthermore, the differences of results by different authors, for example in Ref. 23, from theirs are quite large in some states. In this respect we think that it is quite reasonable to replace the 2π exchange contribution by simple poles of σ and ρ . In this treatment the calculation, i.e., the lowest order calculation, has intrinsically no ambiguity. Furthermore, our OBEP's with fewer adjusted parameters produce better fits. We note here also that the pole description by σ and ρ can be quite a good ap-

proximation to the sum of the uncorrelated (or the continuum) 2π exchange and the correlated 2π exchange as shown by Furuichi.²³ The actual mass distribution of the uncorrelated 2π exchange should be broad. However, it can be a good mathematical approximation to replace the mass distribution by an appropriate sum of δ -function distributions, as argued for the case of the ω . For the $I=J=0$ exchange component we use six δ functions corresponding to the σ and S poles and four poles for the regularization. However, in our opinion, the real significance of the OBE model will be understood in the future in terms of a more fundamental theory such as quark physics than dispersion theory based on πN and $\pi\pi$ dynamics. The one- π , one- ρ , and one- ω exchanges correspond to one quark-antiquark pair exchange and the one- σ exchange, presumably to exchange of the quark-antiquark pair³² in the topological diagram of quark dynamics.

The Bonn group³³ has recently modified OBEP with an eikonal meson form factor to achieve fits to the 1969 Livermore phase parameters.⁷ Since the newest phase parameters^{5,6} differ substantially from the Livermore parameters and have approximately one-half the error bars, their value, 2.77, for the χ^2 value/data which was obtained with respect to the Livermore phase parameters is probably much larger if tested against new data.

As shown by one of us (T.U.),²⁴ the damping factor introduced in this paper can be related to the structure of the vector mesons. He described the structure by introducing space-time extension into the vector meson, which is represented by a bilocal field.²⁴ This has two kinds of coordinates, corresponding to the barycentric and relative coordinates. Imposing appropriate conditions on the bilocal field, he showed that the amplitude due to the exchange of the bilocal vector-meson field gives the local vector-meson exchange amplitude at low energies $E_{1ab} \ll m$, while that amplitude tends to the Reggeized vector-meson exchange amplitude at very high energies $E_{1ab} \gg m$. Thus the damping factor corresponding to the power-law behavior of the Regge pole amplitude comes out consistent with the OBE model at low energies. The calculation of the nucleon-nucleon interaction using this formalism is complicated. In this paper, therefore, we have adopted a simple parametrization which satisfies the features of this formalism both at low energies and at high energies, which has experimental support, that is, the OBE model for low energies and the Regge pole model for high energies.

In this connection, it is interesting that Yonezawa has recently found considerable improvements in fits to data by introducing the Regge pole behavior into his OBE model, though his method is quite dif-

ferent from that presented in this paper.³⁴

As a companion work to this paper, we have developed an updated version of the corresponding nonrelativistic OBEP in r space, which has been made to fit data up to 325 MeV.^{35,36} Though in this nonrelativistic work we have made considerable improvement over older models, some deviations from data at 325 MeV in the 1S_0 , 1D_2 , and 3D_2 states are recognized. The main reason for these deviations is apparently in the nonrelativistic approximation that ignores the terms of the order of (p/m) .⁴ We have no problem with such terms in this relativistic version since higher order kinematics is naturally included. However, we can show in the nonrelativistic models that a modification of the velocity-dependent term by introducing the phenomenological term of the order of $(p/m)^4$ leads to improvement at 325 MeV.³ Perhaps we should recognize that the significance of the nonrelativistic models is in providing an intuitive picture of nuclear forces and as a useful tool for nuclear problems where the phenomena in the normal state concern primarily $p \lesssim 300$ MeV/ c .

In this regard the improvements in this work of models II, III, and IV with respect to model I might have a simple nonrelativistic interpretation. It would appear that the approximate cancellation of the static attractive interaction from scalar-meson exchange by the static repulsive interaction from vector-meson exchange⁹ becomes less complete at higher energies. Thus at higher energies the intrinsic strength of the nuclear interaction implicit in the large coupling constants becomes more manifest. It is well known that these strong interactions are more fully manifest in the $N-\bar{N}$ interaction where the ω meson contributes an attractive interaction (since its G parity is negative).

In final conclusion and summary, this paper has presented markedly improved descriptions with 10 or 11 parameters of the $N-N$ interactions defined by most current experimental data up to 325 MeV in all states and up to 515 MeV in most states except a few states mentioned in Sec. V. At present, it is not clear whether these discrepancies are due to an insufficiency of our models or due to the shortage of experimental information for the phase shift analyses, except the discrepancies in the $\delta(^1D_2)$ and $\delta(^3F_3)$ at 515 MeV. These two may be connected with mechanisms other than that of OBEP. The damping factor for the vector meson and/or the enhancement factor for the scalar meson introduced in this paper lead to a remarkable improvement in fits considering that only one additional parameter is employed. Therefore, we believe that this indicates a good direction to pursue in attempts to unify the models for low energy with the established high energy theory. Finally, since

recent experimental data have revealed some deficiency in the Livermore X phase parameters, to which most of the currently available potentials refer, we believe our potentials, referring to the new data, might be useful in applications to other nuclear and particle processes.

We would like to thank Dr. R. A. Arndt, Dr. J. A. Edgington, Dr. P. Signell, Dr. R. Hess, and Dr. D. H. Fitzgerald for prepublication copies of their recent data or phase shift analyses, Dr. Fred Riewe for helpful discussions, and the Research Council of the University of Florida for computational funds.

APPENDIX

In Table IV we show the phase parameters for the χ^2 test and the ones to which we fitted our model by optimizing the corresponding χ^2 value. The latter set consists of phase parameters and error bars at 1, 25, 150, and 325 MeV which are the same as those for the χ^2 test except for the cases discussed below. This set is adopted for the following physical and technical reasons. As is well known, the ϵ_1 , $\delta(^3S_1)$, and $\delta(^1S_0)$ parameters are of particular importance in nuclear binding. Therefore we emphasize these parameters by giving smaller error bars at 325 MeV than those for the χ^2 test. In our models the ϵ_1 is strongly correlated with the $\delta(^1D_2)$, $\delta(^3P_2)$, and $\delta(^3D_2)$ parameters. Therefore we use the smaller error bars also for these phase parameters at 325 MeV to retain good fits. Another advantage of using the smaller error bars is that their use leads to better fits at 420 and 515 MeV without involving the phase parameters at these energies in the optimization procedure. A smaller error bar for $\delta(^3P_0)$ at 150 MeV is used to obtain a good fit at 100 MeV without involving the phase parameter at this energy in the optimization procedure.

In order to get fits of approximately 1% accuracy to the scattering lengths and the effective ranges we use also smaller error bars of $\frac{1}{6}$ and $\frac{1}{9}$ of those for the χ^2 test for the 1S_0 and 3S_1 phase shifts, respectively, at 25 MeV. At 1 MeV we use the data (the energy-dependent solution) given by AHR with error bars small enough to provide fits with 1% accuracy to the low energy parameters.

As is stated in Sec. IV we implicitly seek a fit to the deuteron quadrupole moment by fitting the ϵ_1 parameter at 1 MeV. For this parameter at 1 MeV, however, the energy-dependent solution in AHR⁴ is not reliable because this solution gives a negative value to the ϵ_1 parameter at 50 MeV, though the latest data³ require a positive value. In this situation we use the result of the Ueda-

TABLE IV. The data for χ^2 test (upper) and $\bar{\chi}^2$ test (lower). The asterisk indicates the same figure with that in the upper side.

Energy	1	25	50	100	150	200	325
1S_0		50.64 ± 0.37	40.37 ± 0.27	25.58 ± 0.46	15.88 ± 0.49	8.37 ± 0.46	-4.96 ± 1.04
	62.41 ± 0.06	*			*		* 0.50
3P_0		10.36 ± 0.22	13.48 ± 0.34	12.28 ± 1.42	5.43 ± 0.43	-0.56 ± 0.48	-14.15 ± 1.84
		*			* ± 0.14		*
1P_1		-4.49 ± 0.94	-6.04 ± 1.86	-12.64 ± 1.13	-19.83 ± 1.10	-22.16 ± 1.55	-30.70 ± 4.80
		*			*		*
3S_1		79.89 ± 0.88	61.72 ± 0.49	42.43 ± 0.59	27.04 ± 0.55	16.81 ± 1.11	-0.49 ± 3.20
	147.81 ± 0.09	* 0.10			*		* ± 0.20
3P_1		-5.93 ± 0.12	-9.27 ± 0.15	-14.68 ± 0.26	-18.80 ± 0.14	-22.53 ± 0.28	-31.97 ± 1.20
		*			*		*
3D_1		-2.83 ± 0.42	-6.51 ± 0.23	-12.18 ± 0.38	-14.95 ± 0.42	-17.64 ± 1.07	-26.50 ± 1.26
		*			*		*
ϵ_1		0.71 ± 0.84	2.90 ± 1.90	0.07 ± 0.96	4.30 ± 0.63	5.99 ± 0.68	7.80 ± 1.20
	0.127 ± 0.001	2.18 ± 0.03			*		* ± 0.20
1D_2		0.86 ± 0.03	1.82 ± 0.06	4.06 ± 0.13	5.68 ± 0.08	7.36 ± 0.13	9.62 ± 0.64
		*			*		* ± 0.12
3P_2		2.90 ± 0.05	6.54 ± 0.08	11.62 ± 0.18	15.42 ± 0.09	16.91 ± 0.19	18.01 ± 1.09
		*			*		* ± 0.50
3D_2		4.29 ± 0.77	10.29 ± 0.30	16.18 ± 0.74	22.46 ± 0.50	25.45 ± 0.76	23.75 ± 1.05
		*			*		* ± 0.30
3F_2		0.11 ± 0.50	0.32 ± 0.50	0.73 ± 0.50	1.11 ± 0.18	1.15 ± 0.26	0.81 ± 0.42
		*			*		*
ϵ_2		-0.95 ± 0.50	-1.87 ± 0.07	-3.00 ± 0.12	-3.11 ± 0.06	-3.09 ± 0.13	-2.85 ± 0.25
		*			*		*

Green 1 potential.¹⁵ This potential reproduces well the deuteron properties (the binding energy, the quadrupole moment, and the D -state probability) and the low energy parameters in the 3S_1 state, which are all closely connected with the ϵ_1 parameter. Therefore, as far as the ϵ_1 parameter at 1 MeV is concerned, we think that the result of the Ueda-Green 1 potential is more reliable than the energy-dependent solution in AHR which does not involve an analysis of the deuteron. For sim-

ilar reasons we also use the result of the Ueda-Green 1 potential at 25 MeV. However, even if one would use the AHR solution ($0.71^\circ \pm 0.84^\circ$) at this energy, one should find no appreciable change in our result. The error bars of the ϵ_1 parameter at 1 and 25 MeV are also chosen to obtain fits to the deuteron quadrupole moment with 1% accuracy. The test against this special set of the phase parameters is called the χ^2 test. The minima of the χ^2 value are obtained by the method in Ref. 37.

*On leave, Osaka University, Osaka, Japan.

¹J. A. Edgington, in *Nucleon-Nucleon Interactions—1977*, edited by D. F. Measday, H. W. Fearing, and A. Strathdee, (American Institute of Physics, New York, 1978).

²D. Besset *et al.*, Ref. 1.

³D. H. Fitzgerald *et al.*, Ref. 1.

⁴R. A. Arndt, R. H. Hackman, and L. D. Roper, Phys. Rev. C **15**, 1002 (1977).

⁵R. A. Arndt, Ref. 1 and private communication.

⁶P. Signell (unpublished).

⁷M. H. MacGregor, R. A. Arndt, and R. M. Wright, Phys. Rev. **182**, 1714 (1969).

⁸R. E. Seamon, K. A. Friedman, G. Breit, R. D. Haraeg, J. M. Holt, and A. Prakash, Phys. Rev. **165**, 1579 (1968).

⁹A. E. S. Green, Phys. Rev. **73**, 519 (1948); **75**, 1926 (1949); **76**, L870, A460 (1949); see also Science **169**, 933 (1970).

¹⁰A. E. S. Green, F. E. Riewe, M. L. Nack, and L. Miller, in *Proceedings of the International Symposium on Present Status and Novel Developments in the Nuclear Many-Body Problem, Rome, 1972*, edited by F. Calogero and C. Ciofi Degli Atti (Editrice Compositori, Bologna, 1973).

¹¹S. Sawada, T. Ueda, W. Watari, and M. Yonezawa, Prog. Theor. Phys. **28**, 991 (1962); **32**, 380 (1964); R. A. Bryan, C. R. Dismukes, and W. Ramsay, Nucl. Phys. **45**, 353 (1963).

¹²S. Ogawa, S. Sawada, T. Ueda, W. Watari, and M. Yonezawa, Prog. Theor. Phys. Suppl. **39**, 140 (1967).

¹³T. Ueda, in *Proceedings of the International Symposium*

- on *Present Status and Novel Developments in the Nuclear Many-Body Problem, Rome, 1972*, edited by F. Calogero and C. Ciofi Degli Atti (Editrice Compositori, Bologna, 1973).
- ¹⁴A. E. S. Green and T. Sawada, Nucl. Phys. B2, 276 (1967); Rev. Mod. Phys. 39, 594 (1967).
- ¹⁵T. Ueda and A. E. S. Green, Phys. Rev. 174, 1304 (1968).
- ¹⁶T. Ueda and A. E. S. Green, Nucl. Phys. B10, 289 (1969).
- ¹⁷A. Gersten, R. H. Thompson, and A. E. S. Green, Phys. Rev. D 3, 2076 (1971); 3, 2069 (1971).
- ¹⁸T. Ueda, M. L. Nack, and A. E. S. Green, Phys. Rev. C 8, 2061 (1973).
- ¹⁹T. Ueda, Phys. Rev. Lett. 26, 288 (1971); Prog. Theor. Phys. 45, 1527 (1971).
- ²⁰M. Kikugawa, S. Sawada, T. Ueda, W. Watari, and M. Yonezawa, Prog. Theor. Phys. 37, 88 (1967).
- ²¹A. E. S. Green, M. H. MacGregor, and R. Wilson, editors, Rev. Mod. Phys. 39, 495 (1967).
- ²²*Nucleon-Nucleon Interactions—1977*, (see Ref. 1).
- ²³S. Sato and T. Ueda, Prog. Theor. Phys. 44, 419 (1970); *ibid.* 47, 1235 (1972).
- ²⁴T. Ueda, Prog. Theor. Phys. 47, 572 (1972); 48, 2276 (1972).
- ²⁵S. Furuichi, Prog. Theor. Phys. Suppl. 39, 190 (1967); S. Furuichi, H. Kanada, and K. Watanabe, Prog. Theor. Phys. 44, 711 (1970); S. Furuichi, report of Center for Nuclear Research, Osaka University, 1976 (unpublished).
- ²⁶R. A. Arndt, Phys. Rev. 165, 1834 (1968); H. Suzuki, Prog. Theor. Phys. 54, 143 (1975).
- ²⁷I. P. Auer *et al.*, Phys. Lett. 70B, 475 (1977); N. Hoshizaki, Prog. Theor. Phys. 58, 716 (1977).
- ²⁸T. Ueda, Osaka University Report No. OUAM 78-1-1 (unpublished); Prog. Theor. Phys. 59, No. 2 (1978).
- ²⁹S. C. C. Ting, in *Proceedings of the Fourteenth International Conference on High Energy Physics, Vienna, 1968*, edited by J. Prentki and J. Steinberger (CERN, Geneva, 1968), p. 3; J. Binstock and R. A. Bryan, Phys. Rev. D 4, 1341 (1971).
- ³⁰S. R. Deans and W. G. Holladay, Phys. Rev. 165, 1886 (1968).
- ³¹R. Vinh Mau, the same proceedings as Ref. 1; in *Mesons in Nuclei*, edited by M. Rho and D. Wilkinson (unpublished).
- ³²T. Ueda, T. Sawada, and S. Takagi, in *Few Body Dynamics, Proceedings of the Seventh International Conference on Few Body Problems in Nuclear and Particle Physics, Delhi, 1976*, edited by A. N. Mitra, I. Slaus, V. S. Bhoosin, and V. K. Gupta (North-Holland, Amsterdam, 1976).
- ³³K. Hollinde and R. Machleidt, Nucl. Phys. A256, 479 (1976).
- ³⁴M. Yonezawa, private communication; Y. Susuki, Prog. Theor. Phys. 49, 541 (1973).
- ³⁵A. E. S. Green, T. Ueda, and F. E. Riewe; the same proceedings as Ref. 1.
- ³⁶T. Ueda, F. E. Riewe, and A. E. S. Green, Phys. Rev. C 17, 1763 (1978).
- ³⁷M. A. Melkanoff, J. Raynal, and T. Sawada, UCLA and USC Joint report, 1965 (unpublished).